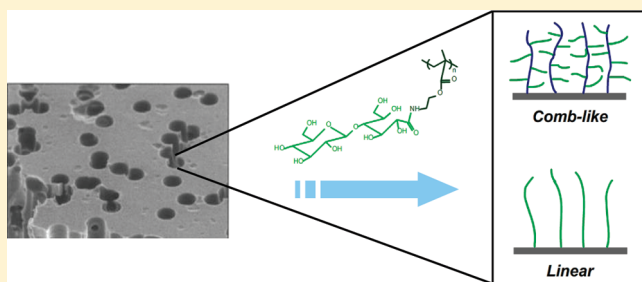


Cylindrical Membrane Pores with Well-Defined Grafted Linear and Comblike Glycopolymer Layers for Lectin Binding

Qian Yang and Mathias Ulbricht*

Lehrstuhl für Technische Chemie II, Universität Duisburg-Essen, 45117 Essen, Germany

ABSTRACT: Glycopolymers with well-defined linear or comblike structure were grafted to poly(ethylene terephthalate) (PET) track-etched membrane surface by surface-initiated atom transfer radical polymerization (ATRP). Bromoalkyl initiator was directly immobilized onto PET membrane surface, and the ATRP of 2-lactobionamidoethyl methacrylate (LAMA) was then carried out to yield the grafted linear glycopolymer. Comblike poly(LAMA) was constructed on PET membrane by a two-step sequence. First, ATRP of 2-hydroxyethyl methacrylate (HEMA) was initiated from the PET surface, and alkyl bromide was then immobilized to poly(HEMA) chains. The initiator-immobilized poly(HEMA) served as a surface tethered macroinitiator for the ATRP of poly(LAMA) and resulted in comblike poly(LAMA) branches. The ATRP conditions for both LAMA and HEMA were optimized, and the thus-established grafting was well controlled. The dry layer thickness (DLT) of grafted polymers was deduced from results of capillary flow porometer measurements. Effective hydrodynamic layer thickness was estimated from pure water permeability. Data revealed that the grafted linear poly(LAMA) and poly(HEMA) had relatively low chain density and exhibited a collapsed coil conformation in dry state. After grafting of poly(LAMA) chains to poly(HEMA) this collapse was significantly hindered by the steric influence of poly(LAMA) branches on the poly(HEMA) main chains, and more than 3 times increase in DLT could be observed. Nonspecific protein binding, studied with bovine serum albumin, was very low for membranes with grafted linear poly(LAMA) while no adsorbed protein could be detected for the comblike poly(LAMA) architecture. Both membranes were then used for binding of peanut agglutinin, a lectin specifically binding to galactose. Under conditions where protein could only diffuse into the membrane pores, comblike poly(LAMA) showed only slight enhancement of binding capacity in comparison with the linear poly(LAMA). However, with convective flow through the membranes, binding capacity of the comblike poly(LAMA) layer was significantly increased and a capacity up to 23.6 mg/cm³ was achieved. Specific lectin binding with high capacities, corresponding to 3-dimensional protein stacking in the grafted layers, could be confirmed.



INTRODUCTION

Carbohydrates dominate the outmost surface of cell membranes and play a major role in many recognition events.¹ It has been proven that recognition is key to a variety of biological processes and the first step in numerous phenomena based on cell–cell interactions, such as blood coagulation, immune response, viral infection, inflammatory reaction, and cellular signal transfer.^{2–4} These recognition processes are thought to proceed by specific carbohydrate–protein interactions. Glycotechnology has been widely accepted as one of the most important tools for a variety of biomedical applications, e.g., for development of receptor blockers for virus or bacteria inhibition,^{5,6} for gene delivery,^{7,8} and to create scaffold materials for tissue engineering.^{9,10} Despite the importance of the carbohydrate–protein interactions and their high specificity, the affinity between these proteins and simple (monomeric) sugar moieties is low ($K_a = 10^3$ – 10^4 M^{−1}).¹¹ Though the mechanism has not been fully understood, it is clear that the presentation of sugar groups on an appropriate scaffold creates a multivalent display that can efficiently mimic the mode of affinity enhancement in nature, resulting in higher affinities than expected from the addition of the individual interactions; this is called the glycoduster effect.^{12–14}

In order to enhance the carbohydrate–protein binding affinity, efforts have been made to achieve multiple sugar clusters on

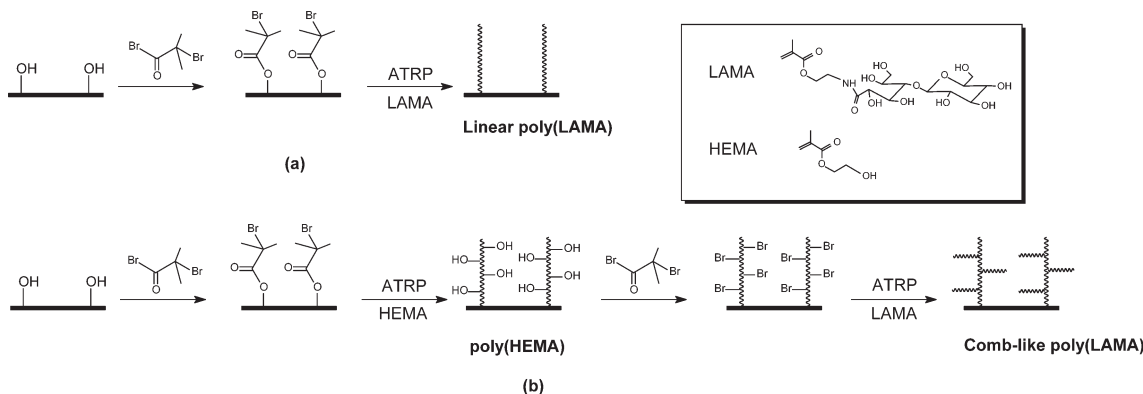
different types of glycoligands.^{15–22} Among such ligands, synthetic polymers (linear, comblike, and dendritic) bearing sugar residues, so-called glycopolymers, have gained special attention. In the past decade, a great number of glycopolymers have been synthesized as reviewed by Wang et al.,²³ Ladmiral et al.,²⁴ or Okada et al.²⁵ and more recently by Miura et al.²⁶ and Voit et al.²⁷ These glycopolymers with various architectures are emerging as an important tool to mimic multivalent ligands in the nature and to perform similar functions in recognition events;²⁸ potential advantages are the very high valency, the ease in controlling the macromolecular structure, and the option to vary the structure of the displayed sugar ligands. In addition, the flexibility of polymer chains is also beneficial for the interaction by fitting to the secondary structure of relevant proteins which are always oligomeric and hence have several carbohydrate binding sites.^{29,30} Moreover, compared to carbohydrate clusters obtained by sugar-ended self-assembled monolayers (SAMs), glycopolymers turn the 2-dimensional binding to a 3-dimensional binding and could potentially significantly increase the protein binding capacity.

Received: November 15, 2010

Revised: January 17, 2011

Published: February 08, 2011

Scheme 1. Schematic Representation for the Grafting of Linear and Comblike Poly(LAMA) on Track-Etched PET Membranes



In recent years, affinity-based membrane adsorbers have attracted great interest and proved to be a promising technique in many fields such as protein separation,³¹ antibody purification,³² and virus capture.³³ Interactions involved in affinity membrane adsorbers are requested to be highly specific, and typical biologic interrelated pairs such as antibody–antigen, protein A/G–IgG, and carbohydrate–protein are good candidates for this purpose. Previous studies showed that glycopolymers immobilized on solid substrate surface have the ability to selectively capture lectins, viruses, and bacteria from solutions or mixtures.^{34–37} Immobilizing glycopolymers to a porous membrane surface can lead to a special affinity adsorber which combines the advantages of high selectivity of carbohydrate–protein interaction and the high specific surface area of the membrane. In order to maximize the capture capacity, all binding sites in the membrane adsorber should be easily accessible within the residence time. Therefore, microfiltration membranes with an isotropic cross section are preferred, but normally they have only more or less coherent pores in spongy membrane morphology. Also, commercial membrane adsorbers have a rather complex pore structure.³⁸ In contrast, track-etched membranes (TEM) with uniform cylindrical pores fulfill this requirement very well. It is relatively easy to achieve an even surface coverage of the pore walls.³⁹ Moreover, measuring the effective thickness of the polymer layer is possible by means of permeability measurements and calculations based on simple pore flow models.⁴⁰ In our previous work,^{40–42} TEM made from poly(ethylene terephthalate) (PET) had been successfully used as a versatile tool to investigate polymers brushes in pores via various grafting techniques and the effects on a material's function. Also, protein binding selectivity and capacity of a membrane adsorber grafted with polymer chains featuring multivalent amino acid-selective groups have been analyzed with PET TEM as base material.⁴³ Knowledge gained from such studies can then be transferred to membranes with higher specific surface area but more complex pore morphology.⁴⁴

Herein, we report a study on construction of linear and comblike glycopolymers on the entire pore surface of PET TEM (Scheme 1). Atom transfer radical polymerization (ATRP) of 2-lactobionamidoethyl methacrylate (LAMA) was initiated directly from the initiator immobilized on PET membrane surface to yield the linear chains. For the comblike structure, poly(2-hydroxyethyl methacrylate) (poly(HEMA)) was first grafted, and then the hydroxyl groups were used to link the ATRP initiator for subsequent initiation of comblike poly(LAMA) chains. Taking advantage of ATRP, the grafting processes of both poly(HEMA) and poly(LAMA) were well controlled. The dry layer thickness was monitored by capillary flow porometer

measurement, and water flux measurement revealed the changes of the grafted layers in hydrated state. Both linear and branched poly(LAMA) grafted PET membranes were then used for lectin binding, and comparisons were made between static (no convective flow through the TEM) and dynamic conditions (flow-through conditions).

EXPERIMENTAL SECTION

Materials. PET TEM with nominal pore diameter of 400 nm and a thickness of 23 μm were purchased from Oxyphen GmbH (Dresden, Germany). All membrane samples used in this study were cut from large sheets into circular specimen with a diameter of 25 mm. LAMA was synthesized in our lab as described in the literature;⁴⁵ the structure and purity had been confirmed by ^1H and ^{13}C NMR spectroscopy as well as elemental analysis. Acetonitrile was purified by refluxing with boric anhydride and distillation before use. Copper(I) bromide (Aldrich, 99.999%), copper(I) chloride (Aldrich, 99.995+%), copper(II) bromide (Acros, 99+%), and copper(II) chloride (Aldrich, 99.999%) were used without further purification. *N*-Methylpyrrolidone (NMP, Aldrich), 2-bromo-2-methylpropionyl bromide (BMPB, Aldrich), triethylamine (TEA, Aldrich), 2,2'-bipyridine (Bpy, Aldrich), 4-(*N,N*-dimethylamino)pyridine (DMAP, Fluka), *N,N,N',N',N'*-pentamethyldiethylenetriamine (PMDETA, Fluka), and methanol were used as received. Peanut agglutinin was from Vector Laboratories Inc., and bovine serum albumin (BSA) was from MP Biomedicals Inc. BCA protein assay (Thermo Scientific) was used for protein concentration determination. The water used in all syntheses and measurements was from a Milli-Q system.

Characterizations. Pore size and its distribution of membranes in dry state were analyzed with a PMI capillary flow porometer (Porous Materials, Inc., Ithaca, NY). The gas flow was measured as a function of the transmembrane pressure, first through the dry membrane and then after wetting the membrane with 1,1,2,3,3,3-hexafluoropropene ("Galwick", PMI, surface tension 16 dyn cm^{-1}). The pore size distribution was then deduced from the comparison of the two experiments by using the PMI software. The dry layer thickness on the pore walls (DLT) was obtained as the difference between the pore radius of the unmodified membrane and the pore radius of the grafted membrane.

Measurements of pure water permeability in thermostated Amicon cells (Millipore, MA) as well as calculations of reduction of pore diameter (for modified membranes) were also done according to the earlier described procedures.⁴⁰ In order to ensure that grafted glycopolymer layers were completely swollen in water, the membrane samples were equilibrated in water for at least 30 min before starting the experiments. Briefly, permeability resulted from dividing the flux by the transmembrane pressure, and the pore size of the membrane was calculated from the permeability data by using the

Hagen–Poiseuille equation:

$$\frac{V}{\Delta t} = \frac{\pi \Delta p r^4}{8 \eta L}$$

where V is the volume of the permeate relating to a single cylindrical membrane pore, Δt is the time interval, Δp is the transmembrane pressure, r is the pore radius, η is the viscosity of water, and L is the capillary length (i.e., the membrane thickness). This equation is valid assuming a cylindrical geometry of the membrane pores and equal size of all pores. First, hydrodynamic pore radius and pore density of unmodified membrane were calculated from the water permeability and capillary flow porometry data. Then, the hydrodynamic thickness of the grafted layer on the pore wall (HLT) was obtained as the difference between the pore radius of the unmodified membrane and the pore radius of the grafted membrane.

Construction of Linear and Comblike Poly(LAMA) on PET Membrane. *Initiator Immobilization.* Immobilization of the ATRP initiator onto the PET TEM was achieved by the reaction between BMPB and hydroxyl groups on the PET surface. The membrane samples were put in a vessel with 10 mL of freshly dried acetonitrile containing DMAP (5 mM) and TEA (10 mM), and then 100 μ L of BMPB was added. The vessel was then sealed and put on a shaker. After reaction for 2 h at room temperature, membranes were taken out, rinsed with acetonitrile, water, and ethanol, and then dried in vacuum oven at 40 °C overnight.

Linear Poly(LAMA) on PET Membrane. Initiator-immobilized membrane samples were put in a Schlenck flask equipped with rubber stoppers, and the flask was sealed. Then, the flask was evacuated and backfilled with argon three times. LAMA and Bpy were dissolved in 30 mL of water (or NMP) and purged with nitrogen for 30 min. Then, copper(I) bromide was added to the solution under drastic stirring and argon stream. In some cases, a certain amount of copper(II) bromide was also added to the system. Subsequently, reaction solution was cannulated into the flask (6 mL for each sample), and the reaction mixture was incubated at room temperature for a predetermined time. After ATRP reaction, a quenching solution was used to stop the polymerization. The membranes were quickly removed from the Schlenck flask and immersed in 50 mL of 1:1 (v/v) methanol/water solution of 250 mg of copper(II) bromide and 625 μ L of PMDETA. A water–methanol–ethanol washing sequence was then used to clean the membranes. After drying in vacuum oven at 40 °C overnight, the degree of grafting, DG (μ g/cm²), was calculated by following equation:

$$DG = \frac{W_1 - W_0}{A_m}$$

where W_0 is the mass of the unmodified membrane and W_1 is the mass of the membrane after modification and drying. A_m represents the area of the membrane (4.9 cm² in this study). The membrane samples were weighed using the balance GENIUS (accuracy: ± 10 μ g) from Sartorius (Germany). Except for the screening experiments to find controlled polymerization conditions, all the other preparations were repeated for at least three times, and here the corresponding average values and standard deviations are reported.

Comblike Poly(LAMA) on PET Membrane. For construction of comblike poly(LAMA) layer on PET membrane surface, a two-step process was applied. As shown in Scheme 1b, poly(HEMA) was first grafted on the PET membrane surface by ATRP. For the ATRP of HEMA, Bpy, copper(I) chloride and copper(II) chloride were used as catalyst system in a 1:1 (v/v) methanol/water mixture as solvent. The DG of poly(HEMA) was determined according to the same method used for linear poly(LAMA). Then the hydroxyl groups on poly(HEMA) served as anchor sites for ATRP initiator immobilization; immobilization was performed using the same method as described for linear poly(LAMA). Afterward, ATRP of LAMA was initiated from grafted poly(HEMA) chains under the same conditions used for linear poly(LAMA) grafting. The DG of branched poly(LAMA) was

calculated by dividing the weight difference before and after poly(LAMA) grafting by the membrane area (cf. above).

Protein Binding. Lectin Recognition. Lectin binding experiments were carried out without (“static binding”) and with flow through the membranes (“dynamic binding”). Throughout, a 1 g/L PNA solution in HEPES buffer solution (10 mM, pH = 7.36), containing 0.1 mM CaCl₂ and 0.15 M NaCl, was used. For the static binding, membranes with diameter of 13 mm were immersed in HEPES for 30 min to prewet. Then each sample was put into a vessel, and 5 mL of PNA solution was added. The samples were incubated at 25 °C for 4 h with slight shaking. For the dynamic binding, membranes with diameter of 25 mm were sealed in a membrane holder and 10 mL of PNA solution was forced through the membrane at a rate of 0.1 mL/min by using a syringe pump. The permeate solution was then collected. The amount of bound PNA was determined by measuring spectrophotometrically the difference between the concentrations of PNA in the solution before and after contact with the membranes. The BCA protein assay with the typical microplate procedure described in the instruction book has been applied using the Microplate Reader (Bio-Tek Instruments Inc.).

BSA Adsorption. Membranes with diameter of 13 mm were immersed in phosphate buffer solution (PBS, 10 mM, pH = 7.36) for 30 min to prewet. Then each sample was put into a vessel containing 5 mL of BSA solution (1 g/L in 10 mM PBS, pH = 7.36) at 25 °C for 4 h with slight shaking. Analysis of bound BSA was done as described above for PNA.

RESULTS AND DISCUSSION

Linear Poly(LAMA) Grafting. The reaction sequence for the grafting of linear poly(LAMA) to the membrane surface, including immobilization of the ATRP initiator and graft copolymerization, is summarized in Scheme 1a. The BMPB was immobilized to the hydroxyl groups on the membrane surface directly and led to a lower initiator density compared to the methods which were used in previous studies,^{40–42} which included a pretreatment step to increase hydroxyl group density. The initiator immobilization conditions had been developed and proven to proceed at high conversion on the one hand; most important, the cylindrical pore morphology with very narrow size distribution of the PET TEM remained unchanged on the other hand.⁴¹ The pore diameter of the PET TEM before and after modification was determined by permoporometry. The pore diameter of the unmodified membrane batch used in this study was ~ 687 nm; this was much higher than the value provided by the manufacturer. This was similar to previous studies, and the possible reason, overetching during production, had been discussed before.^{40–42}

Then, the graft copolymerization of LAMA was initiated from PET membrane surface, and the ATRP conditions were optimized. Water and NMP were used as solvents for ATRP of LAMA. The maximum concentrations of LAMA which could be achieved in water and NMP at room temperature were 0.1 and 0.3 M, respectively. Compared with water, NMP is a less polar solvent and showed a slow ATRP rate even with a much higher monomer concentration, which was 3-fold that in water (see Figures 1 and 2).

The high dielectric constant of water probably affects the structure and the activity of the catalyst.^{46,47} Matyjaszewski et al.^{48,49} also suggested that in aqueous media the most probable structure of the catalytic species is the monocationic $[\text{Cu}(\text{I})(\text{bpy})_2]^+$ complex with a halide counterion which is much more active than the neutral, binuclear Cu(I) complex with bridging halide ligand which occurs in bulk or nonaqueous ATRP systems. High activity of the Cu(I) complex leads to high polymerization rate. Moreover, the lack of

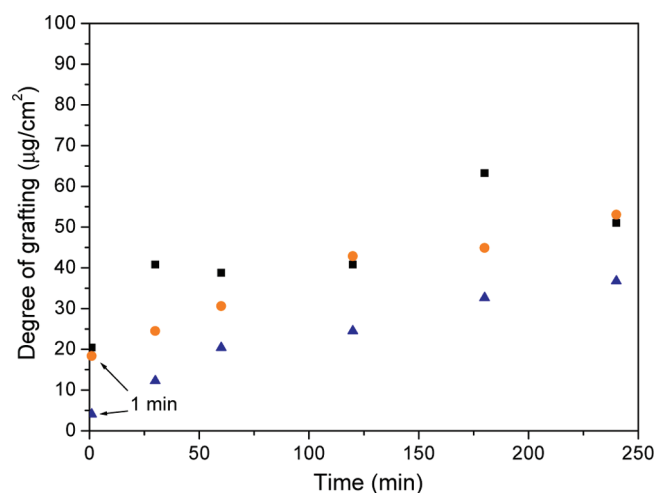


Figure 1. Dependence of poly(LAMA) DG on PET membrane on the surface-initiated ATRP time (solvent: water; monomer concentration: [LAMA] = 0.1 M; molar ratio of the components: (■) [LAMA]/[CuBr]/[Bpy] = 100:1:2, (●) [LAMA]/[CuBr]/[CuBr₂]/[Bpy] = 100:1:0.1:2, (▲) [LAMA]/[CuBr]/[CuBr₂]/[Bpy] = 100:1:0.25:2).

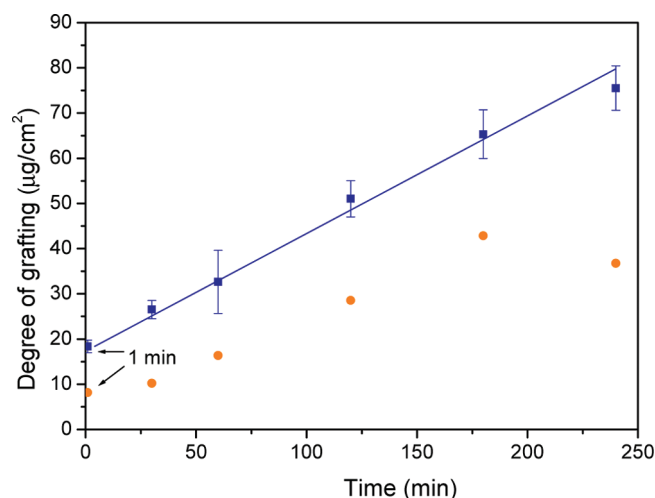


Figure 2. Dependence of poly(LAMA) DG on PET membrane on the surface-initiated ATRP time (solvent: NMP; (■) monomer concentration: [LAMA] = 0.3 M; molar ratio of the components: [LAMA]/[CuBr]/[Bpy] = 100:1:2; (●) monomer concentration: [LAMA] = 0.2 M, molar ratio of the components: [LAMA]/[CuBr]/[Bpy] = 100:1:2).

deactivating Cu(II) complex at the beginning of polymerization made the ATRP equilibrium shift to the active species side and resulted in high radical concentration.⁵⁰ Therefore, as can be seen from Figure 1, even though the monomer concentration was very low in water, a very high ATRP rate was observed and more than 20 $\mu\text{g}/\text{cm}^2$ DG was obtained in 1 min. However, high radical concentration in the initial stage led to significant chain termination, and a short propagating period was found. Cu(II) bromide was then added to the reaction system to provide a high enough concentration of deactivating Cu(II) complex at the beginning of the ATRP.⁵⁰ However, a small amount of Cu(II) could hardly solve this problem, and the polymerization rate remained too high within the first minute. Though the polymerization was slowed down and the polymerization process was more controllable when the Cu(II) concentration was further enhanced, the polymerization rate became too slow, and

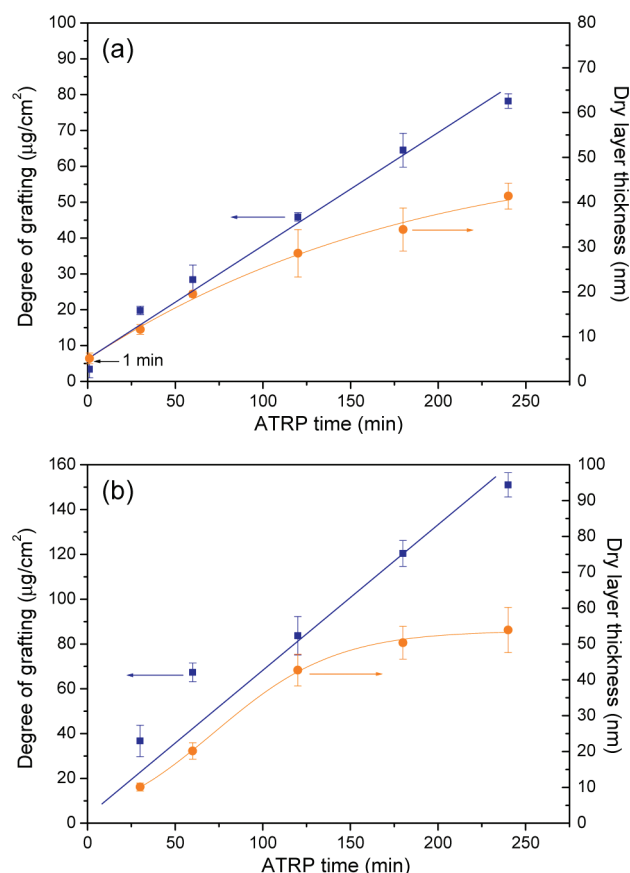
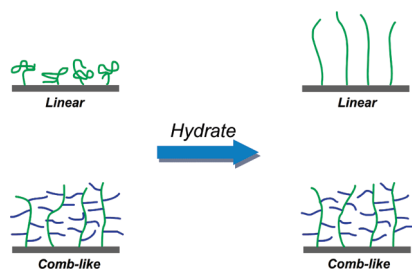


Figure 3. Dependence of DG (■) and dry layer thickness (●) of poly(LAMA) (a) and poly(HEMA) (b) on PET membrane on the surface-initiated ATRP time (LAMA: solvent: NMP; monomer concentration: [LAMA] = 0.3 M; molar ratio of the components: [LAMA]/[CuBr]/[CuBr₂]/[Bpy] = 100:1:0.1:2; HEMA: solvent: water/methanol = 1:1, monomer concentration: [HEMA] = 2 M; molar ratio of the components: [HEMA]/[CuCl]/[CuCl₂]/[Bpy] = 100:0.5:0.2:1.75).

after 4 h the DG was still less than 40 $\mu\text{g}/\text{cm}^2$. Too high polarity and too low solubility of LAMA makes water not a suitable solvent for the ATRP of LAMA. As shown in Figure 2, in NMP the same problem was faced without Cu(II) in the system; however, the polymerization was in a much more controlled manner after the initial stage which might be the result of enhanced solubility and lower polarity. Importantly, the polymerization became well controlled by adding a small amount of Cu(II), and the DG exhibited a linear increase with reaction time (Figure 3). The dry layer thickness of grafted poly(LAMA) was measured and is shown in Figure 3a. The thickness increased with the ATRP time, however, an obvious decline could be observed. This might be ascribed to the relatively low chain density. The exact grafting density was unknown due to well-known experimental problems in analysis for such complex structures. However, the density was certainly much lower than in previous own work using other monomers with the same membranes^{41,42} because no premodification of the PET had been done to increase ATRP initiator density, and the size of LAMA is larger than the one of those monomers used before, probably imposing steric hindrance for initiation. The polymer chains have enough space to collapse in the dry state and most probably exhibited a “mushroom” structure (see Scheme 2). When DG was relatively low, increasing chain length might significantly increase the layer thickness. However, further increase of chain length could only bring volume growth of

Scheme 2. Schematic Diagram Illustrating the Chain Conformations of Linear and Comblike Poly(LAMA) in Dry and Hydrated States



the polymer coil and yielded an effect on layer thickness which was less than proportional with ATRP time, i.e., chain length. Moreover, the polymer–surface interactions may also contribute to the nonlinear increase of dry layer thickness. Because of the low grafting density, grafted macromolecular chain segments had enough space to adsorb on the membrane polymer surface.

Comblike Poly(LAMA) Grafting. To construct comblike poly(LAMA) chains on PET membrane, poly(HEMA) was first grafted to membrane surface by ATRP (cf. Scheme 1b). The ATRP conditions of poly(HEMA) grafting on different substrates have been reported by other groups,^{51–53} and slight changes were made to achieve optimization in this study. As shown in Figure 3b, in the first 4 h, the DG of poly(HEMA) increased linearly with reaction time, indicating a well-controlled polymerization process. The dry layer thickness of the grafted poly(HEMA) also increased with reaction time, and after 4 h about 60 nm polymer layer was achieved. Similar to the case of linear poly(LAMA), the dry layer thickness of poly(HEMA) also showed a nonlinear relationship with ATRP time because of the “mushroom” structure and/or the polymer–surface interaction. Moreover, the slowing down of dry layer thickness increase with ATRP time was even more significant for poly(HEMA) than for poly(LAMA). This could be explained by the difference in side group size. LAMA has a disaccharide pendant group which is much bigger than the hydroxyl group of HEMA and results in a more pronounced steric hindrance. Therefore, poly(LAMA) chains could fold less effectively than poly(HEMA), and a larger dry layer thickness at the same DG was the result.

Grafted poly(HEMA) was then used to attach the ATRP initiator by the reaction between hydroxyl groups and BMPB. The ATRP of LAMA was carried out from these initiator-immobilized poly(HEMA) chains, and comblike poly(LAMA) branches were obtained. As can be seen from Figure 4 for experiments at constant reaction time, the DG of poly(LAMA) increased linearly with the DG of poly(HEMA) in relatively lower DG range, but reduced values were observed when DG of poly(HEMA) was higher than 100 $\mu\text{g}/\text{cm}^2$. This might be ascribed to an increasing hindrance for the diffusion of LAMA into thicker poly(HEMA) layers to reach the propagating chain ends.

To investigate the influence of ATRP time on the DG of comblike poly(LAMA), ATRP initiator was immobilized on poly(HEMA) grafted membranes with similar DG (average DG was $74.8 \pm 6.4 \mu\text{g}/\text{cm}^2$). ATRP of LAMA was then performed under the identical conditions except for the reaction time, and the results are shown in Figure 5. The DG of poly(LAMA) branches increased with the reaction time; however, a significant decline of

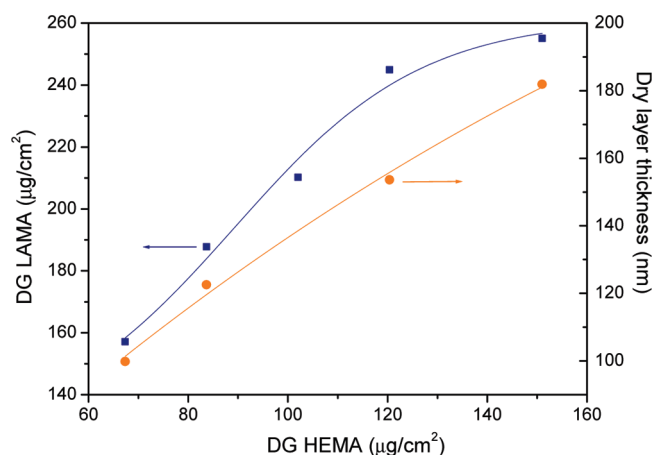


Figure 4. Effect of DG of previously grafted poly(HEMA) on the DG (■) of poly(LAMA) and on the dry layer thickness (●) after poly(LAMA) grafting to yield the comblike architecture (solvent: NMP; monomer concentration: $[\text{LAMA}] = 0.3 \text{ M}$; molar ratio of the components: $[\text{LAMA}]/[\text{CuBr}]/[\text{Bpy}] = 100:1:2$; reaction time: 2 h).

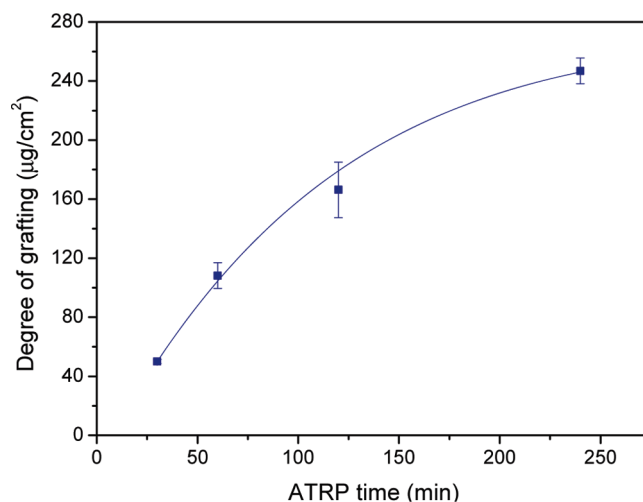


Figure 5. Effect of ATRP time on DG of LAMA from PET membranes with previously grafted poly(HEMA) with similar DG ($74.8 \pm 6.4 \mu\text{g}/\text{cm}^2$) (solvent: NMP; monomer concentration: $[\text{LAMA}] = 0.3 \text{ M}$; molar ratio of the components: $[\text{LAMA}]/[\text{CuBr}]/[\text{Bpy}] = 100:1:2$).

growth rate was found within 4 h. Apparently with increasing ATRP time, the poly(LAMA) branches led to an increasing polymer density in the layer, increasingly hindering the further growth of chain length.

The dry layer thickness of the polymer layer before and after the grafting of poly(LAMA) branches was measured by permoporometry, and results are shown in Table 1. As mentioned before, the dry layer thickness of poly(HEMA) increased with the DG, and then the increase slowed down because of the “mushroom” structure of the polymer chains on the membrane surface. Interestingly, after grafting of poly(LAMA) branches a tremendous jump of the dry layer thickness was observed, and the thickness of the polymer layer after poly(LAMA) grafting was about 3–4 times of that before. This very large increase cannot be the result of reinitiation of the poly(HEMA) chain ends because only 25 nm poly(LAMA) could be obtained directly from PET membrane surface in 2 h under the same ATRP conditions (cf. Figure 3a).

Table 1. Dry Layer Thickness of Poly(HEMA) Layer before and after Grafting of Poly(LAMA) Branches

DG _{HEMA} ^a ($\mu\text{g}/\text{cm}^2$)	DLT _{HEMA} ^b (nm)	DG _{LAMA} ^c ($\mu\text{g}/\text{cm}^2$)	DLT _{LAMA} ^b (nm)
67.4	20.2	157.1	99.8
83.7	42.7	187.8	122.6
120.4	50.4	244.9	153.6
151.0	53.9	255.1	181.9

^a Under the same ATRP conditions with different reaction times. ^b Dry layer thickness; data estimated from gas flow/liquid dewetting permoporometry measurement. ^c Under the same ATRP conditions with the same reaction time (2 h).

This increase of dry layer thickness could be explained with a hindrance of poly(HEMA) chain collapse by poly(LAMA) branches. As shown in Scheme 2, the poly(HEMA) chains became more hydrated and stretched away from the surface with increasing growth of poly(LAMA). Once the poly(LAMA) branches had been grafted, the thus-modified polyHEMA chains could not collapse anymore upon transition into the dry state as the linear chains could (into the mushroom structure), and apparently the chains were, to some extent, still in a stretched conformation. To further confirm this hypothesis, the hydrodynamic layer thickness of the two different grafted layers was measured, and results are shown in Table 2. For the linear poly(LAMA), the ratio between hydrodynamic layer thickness and dry layer thickness increased with increasing DG. This was in line with the “mushroom” structure in the dry state evoked above. In contrast, for the comblike structure, this ratio decreased with the increase of DG of poly(LAMA). Moreover, the membranes used for this measurement had similar DG of poly(HEMA) and were then grafted poly(LAMA) with different DG by changing ATRP time. Thus, the grafting of longer poly(LAMA) promoted the poly(HEMA) main chains to stretch more from the surface so that the difference between dry layer and hydrodynamic thicknesses diminished. This would also be in line with a relatively low grafting density of the poly(HEMA) main chains and a gradual increase of polymer density in the layer along with the growth of the poly(LAMA) branches. Considering the large excess of side groups bearing introduced ATRP initiator, the possible reinitiation of the poly(HEMA) chain ends and grafting of a second poly(LAMA) block can most probably be ignored. It should be noted that the estimated hydrodynamic thickness could also be influenced by a systematic error due to the detailed grafted structure. For linear and comblike structure with short poly(LAMA) branches, the hydrated polymer layer has a lower polymer fraction, and deformation by shear could lead to a lower thickness than for the undisturbed one. In case of comblike structure with longer poly(LAMA) branches, i.e., at higher polymer fraction in the grafted layer, such an effect would be less pronounced. Because the dry layer thickness deduced from the dewetting permoporometry was discussed assuming a heterogeneous topography—isolated collapsed coils at unknown average spacing—no attempt was made to calculate the polymer fraction (or density) in the swollen layers (cf. ref 41). However, most important, all results are in line with a significant influence of the grafted architecture onto layer properties, i.e., polymer fraction and changes upon transition from deswollen to swollen state.

Lectin Binding. The galactose end groups on poly(LAMA) chains can selectively bind to PNA based on the carbohydrate–protein interaction. This interaction is highly specific; however, the affinity for the 1:1 complex is always low. Glycopolymers with sugar side groups well aligned along polymer chains display a

promising clustered sugar ligand system and have been proven to be a very effective way for enhancement of the affinity.

Table 3 shows the results from static binding in which the membranes were immersed in PNA solution and the proteins had to reach the carbohydrate ligands by diffusion. Membranes with grafted linear poly(LAMA) chains showed a clear relationship between DG and amount of PNA binding. With the increase of DG, longer chains were grafted on the surface, and consequently, more binding sites were available for PNA binding. Moreover, linear chains on the membrane surface were flexible, and the polymer layer was loosely packed which made the carbohydrate side groups on the poly(LAMA) chains well accessible for protein. Branching poly(LAMA) chains to a comblike structure offered an easy way to enhance the carbohydrate ligands density, and a much higher DG of poly(LAMA) was achieved in comparison with the linear grafted structure. However, this enhancement failed to yield increased PNA binding under the static incubation conditions; for a very high DG value the bound protein amount showed even a decrease. Considering the results from water permeability measurements, expressed as hydrodynamic layer thickness (cf. Table 2), the core of the cylindrical pores was still free of grafted polymer, and 4 h incubation should be sufficient to reach saturation of the 23 μm long pores with protein by diffusion. Therefore, the results might be ascribed to the steric hindrance for binding in the densely grafted comblike layer structure. To facilitate mass transfer, PNA binding had been performed in flow-through mode. The convective transport of the protein through the pores significantly enhanced protein binding in the branched poly(LAMA) layer while for the grafted linear layer no significant difference had been observed (Table 4). Apparently, the convective flow could also increase the mass transfer through and into the swollen grafted hydrogel layer. The protein binding capacity was normalized by the respective mass of grafted polymer and expressed as mg of protein per mg of grafted polymer (R_{pp} , Tables 3 and 4). The high ratios were in line with a 3-dimensional, “stacked” protein binding in grafted layers with thicknesses in swollen state of up to 200 nm. For the comblike poly(LAMA) grafted PET TEM more than 3 times of increase in R_{pp} and higher R_{pp} values than for linear poly(LAMA) under convective flow conditions indicated the higher availability of the binding sites. Compared with data for commercial membrane adsorbers (23 or 44 mg/cm^3 for lysozyme with two different Sartobind ion-exchanger membranes)³⁸ and results for attempts to improve them by tailored grafting (up to 90 mg/cm^3),⁴⁴ the binding capacity was relatively high considering the very low porosity ($\sim 10\%$) of the PET TEM used in this study. At a porosity of $\sim 70\%$, the commercial materials have about 7 times larger pore fraction per membrane volume; i.e., 7 times higher lectin binding capacities would result when the grafting would be transferred from PET TEM to such macroporous base materials.

BSA Binding. In our previous work,^{35,54–56} other grafted glycopolymers had been demonstrated to effectively recognize lectins with high specificity and, simultaneously, to exhibit outstanding resistance toward nonspecific protein adsorption. Thus, we also used BSA as a nonspecific model protein for the comparison with lectin to investigate the antinonspecific adsorption property of linear and comblike poly(LAMA) on PET TEM (Table 5). The BSA data for linear poly(LAMA) were 1 order of magnitude lower than for the lectin PNA and decreased with increasing DG. For the comblike structure, no BSA adsorption could be detected. In the linear case, the grafted poly(LAMA) layer had a low

Table 2. Comparison of Dry Layer Thickness and Hydrodynamic Thickness of Linear and Comblike Poly(LAMA) Layers

linear poly(LAMA)				comblike poly(LAMA)			
DG _{LAMA} ($\mu\text{g}/\text{cm}^2$)	DLT ^a (nm)	HLT ^b (nm)	R ₁ ^c	DG _{HEMA} / DG _{LAMA} ($\mu\text{g}/\text{cm}^2$)	DLT _{HEMA} / DLT _{LAMA} ^d (nm)	HLT _{LAMA} (nm)	R ₂ ^c
38.7	26.5	60.8	2.3	75.7/49.0	47.3/58.6	146.2	2.5
77.6	42.5	129.1	2.7	71.4/153.1	42.3/102.6	153.6	1.5
87.2	45.2	162.3	3.6	77.6/216.3	45.2/147.8	181.9	1.2

^a Dry layer thickness, data estimated from gas flow/liquid dewetting permporometry measurement. ^b Hydrodynamic layer thickness; data estimated from pure water flux data. ^c For the linear poly(LAMA) $R_1 = \text{HLT}/\text{DLT}$; for comblike poly(LAMA) structure $R_2 = \text{HLT}_{\text{LAMA}}/\text{DLT}_{\text{LAMA}}$. ^d Dry layer thickness measured on poly(HEMA) grafted samples before and after grafting of poly(LAMA) branches.

Table 3. Static Adsorption of PNA onto Linear and Comblike Poly(LAMA) Grafted PET Membrane

polymer structure	poly(LAMA)		PNA binding (mg/cm^3)	R_{pp} ^b (mg/mg)
	degree of grafting, DG ($\mu\text{g}/\text{cm}^2$)	DG ^a (mg/cm^3)		
linear	38.4	16.7	2.8 ± 0.8	0.17
	75.5	32.8	7.7 ± 2.6	0.23
comblike	102.1	44.4	11.4 ± 0.9	0.26
	216.3	94.0	10.2 ± 0.5	0.11

^a Calculated by dividing DG in $\mu\text{g}/\text{cm}^2$ by membrane thickness (0.0023 cm). ^b R_{pp} : ratio between mass of bound protein and grafted polymer mass in same membrane volume (in mg/mg).

Table 4. Dynamic Permeation of PNA through Linear and Comblike Poly(LAMA) Grafted PET Membrane

polymer structure	poly(LAMA)		PNA binding (mg/cm^3)	R_{pp} ^b (mg/mg)
	degree of grafting, DG ($\mu\text{g}/\text{cm}^2$)	DG ^a (mg/cm^3)		
linear	36.7	16.0	3.2 ± 1.0	0.20
	70.7	30.7	8.4 ± 2.3	0.27
comblike	49.0	21.3	7.1 ± 1.1	0.33
	153.1	66.6	23.6 ± 2.9	0.35

^a Calculated by dividing DG in $\mu\text{g}/\text{cm}^2$ by membrane thickness (0.0023 cm). ^b R_{pp} : ratio between mass of bound protein and grafted polymer mass in same membrane volume (in mg/mg).

Table 5. Static Adsorption of BSA onto Linear and Comblike Poly(LAMA) Grafted PET Membrane

polymer structure	poly(LAMA)		BSA adsorption (mg/cm^3)	R_{pp} ^b (mg/mg)
	grafting degree, DG ($\mu\text{g}/\text{cm}^2$)	DG ^a (mg/cm^3)		
linear	38.4	16.7	0.43 ± 0.23	2.6×10^{-2}
	75.5	32.8	0.13 ± 0.09	4.0×10^{-3}
comblike	102.1	44.4	— ^c	—
	216.3	94.0	— ^c	—

^a Calculated by dividing DG in $\mu\text{g}/\text{cm}^2$ by membrane thickness (0.0023 cm). ^b R_{pp} : ratio between mass of adsorbed protein and grafted polymer mass in same membrane volume (in mg/mg). ^c No concentration change in the protein solution before and after incubation with membrane was detected.

grafting density and the membrane surface was not perfectly covered. Therefore, BSA could easily contact the hydrophobic

PET and adsorb to the membrane surface; this interaction was better screened for higher DG. Previously, we had demonstrated that ATRP grafted glycopolymer layers at sufficient grafted density and chain length could minimize nonspecific protein adsorption.⁵⁷ On the other hand, the comblike structure poly(LAMA) formed a much denser hydrated layer on the membrane surface and very effectively prevented the adsorption of BSA. These data confirm that the high lectin binding capacity was achieved with high selectivity because the poly(LAMA) grafted PET TEM exhibited outstanding resistance to nonspecific protein binding.

CONCLUSIONS

Glycopolymers with well-defined linear and comblike structures were successfully grafted from track-etched PET membrane by surface-initiated ATRP. The grafting processes were well controlled. The polymer layer thickness and structure were evaluated by dry layer thickness and hydrodynamic layer thickness measurements making use of the well-defined cylinder pores of the PET TEM. All data can be explained with a relatively low grafting density of the linear poly(LAMA), i.e., a “mushroom” structure. The comblike polymer layer showed a very large increase in dry layer thickness after grafting of the poly(LAMA) branches to the poly(HEMA) main chains which could be ascribed to the obstruction of the collapse of the chains due to the steric hindrance by and among the side branches. Data for hydrodynamic layer thickness are in accordance with this explanation. Only small differences between dry and hydrodynamic layer thicknesses for comblike polymers with the longest poly(LAMA) branches indicated a relatively high polymer density in the swollen layer. While nonspecific protein binding was very low (for linear grafts) or negligible (for the comblike grafted layers), poly(LAMA) grafted PET membrane showed very high binding capacities for PNA under both static and dynamic conditions. 3-Dimensional “stacked” lectin binding in grafted layers with thicknesses in swollen state of up to 200 nm was achieved. The enhancement of sugar density by the comblike structure could only be exploited to full extend under flow-through conditions where the convection increased the protein mass transfer into the grafted layers with relatively high polymer density. These linear and comblike glycopolymers grafted membranes could be very promising for applications such as protein separation and bacteria or virus capture. Further work will focus on adjusting the chain density to achieve optimized lectin binding, and the membranes will be used as the stationary phase in affinity chromatography for protein separation. In our recent work,⁵⁸ linear poly(LAMA) grafted polypropylene membrane has been successfully used for selective capture of bacteria. Hence, increases in both capacity and selectivity could be expected with a

comblike polyLAMA structure also for capturing of other bioparticles such as bacteria.

AUTHOR INFORMATION

Corresponding Author

*E-mail: mathias.ulbricht@uni-essen.de.

ACKNOWLEDGMENT

Alexander von Humboldt foundation, Germany, is thanked for the postdoctoral fellowship of Dr. Qian Yang.

REFERENCES

- (1) Holland, N. B.; Qiu, Y.; Ruegsegger, M.; Marchant, R. E. *Nature* **1998**, *392*, 799–801.
- (2) Gruner, S. A. W.; Locardi, E.; Lohof, E.; Kessler, H. *Chem. Rev.* **2002**, *102*, 491–514.
- (3) Varki, A. *Glycobiology* **1993**, *3*, 97–130.
- (4) Dwek, R. A. *Chem. Rev.* **1996**, *96*, 683–720.
- (5) Hidari, K. I. P. J.; Murata, T.; Yoshida, K.; Takahashi, Y.; Minamijima, Y.; Miwa, Y.; Adachi, S.; Ogata, M.; Usui, T.; Suzuki, Y.; Suzuki, T. *Glycobiology* **2008**, *18*, 779–788.
- (6) Imberty, A.; Chabre, Y. M.; Roy, R. *Chem.—Eur. J.* **2008**, *14*, 7490–7499.
- (7) Prevette, L. E.; Lynch, M. L.; Kizjakina, K.; Reineke, T. M. *Langmuir* **2008**, *24*, 8090–8101.
- (8) Reineke, T. M. *J. Polym. Sci., Part A: Polym. Chem.* **2006**, *44*, 6895–6908.
- (9) Onodera, T.; Niikura, K.; Iwasaki, N.; Nagahori, N.; Shimaoka, H.; Kamitani, R.; Majima, T.; Minami, A.; Nishimura, S. I. *Biomacromolecules* **2006**, *7*, 2949–2955.
- (10) Özyürek, Z.; Franke, K.; Nitschke, M.; Schulze, R.; Simon, F.; Eichhorn, K.-J.; Pompe, T.; Werner, C.; Voit, B. *Biomaterials* **2009**, *30*, 1026–1035.
- (11) Nagahori, N.; Nishimura, S. *Biomacromolecules* **2001**, *2*, 22–24.
- (12) Mammen, M.; Choi, S. K.; Whitesides, G. M. *Angew. Chem., Int. Ed.* **1998**, *37*, 2754–2794.
- (13) Lundquist, J. J.; Toone, E. J. *Chem. Rev.* **2002**, *102*, 555–578.
- (14) Lee, Y. C.; Lee, R. T. *Acc. Chem. Res.* **1995**, *28*, 321–327.
- (15) Benito, J. M.; Gomez-Garcia, M.; Mellet, C. O.; Baussanne, I.; Defaye, J.; Fernandez, J. M. G. *J. Am. Chem. Soc.* **2004**, *126*, 10355–10363.
- (16) Wolfenden, M. L.; Cloninger, M. J. *J. Am. Chem. Soc.* **2005**, *127*, 12168–12169.
- (17) Bandaru, N. M.; Sampath, S.; Jayaraman, N. *Langmuir* **2005**, *21*, 9591–9596.
- (18) Pourceau, G.; Meyer, A.; Chevolot, Y.; Souteyrand, E.; Vasseur, J.-J.; Morvan, F. *Bioconjugate Chem.* **2010**, *21*, 1520–1529.
- (19) Takasu, A.; Iso, K.; Dohmae, T.; Hirabayashi, T. *Biomacromolecules* **2006**, *7*, 411–414.
- (20) Hasegawa, T.; Kondoh, S.; Matsuura, K.; Kobayashi, K. *Macromolecules* **1999**, *32*, 6595–6603.
- (21) Muthukrishnan, S.; Jutz, G.; Andre, X.; Mori, H.; Müller, A. H. E. *Macromolecules* **2005**, *38*, 9–18.
- (22) Muthukrishnan, S.; Mori, H.; Müller, A. H. E. *Macromolecules* **2005**, *38*, 3108–3119.
- (23) Wang, Q.; Dordick, J. S.; Linhardt, R. J. *Chem. Mater.* **2002**, *14*, 3232–3244.
- (24) Ladmiral, V.; Melia, E.; Haddleton, D. M. *Eur. Polym. J.* **2004**, *40*, 431–449.
- (25) Okada, M. *Prog. Polym. Sci.* **2001**, *26*, 67–104.
- (26) Miura, Y. J. *Polym. Sci., Part A: Polym. Chem.* **2007**, *45*, 5031–5036.
- (27) Voit, B.; Appelhans, D. *Macromol. Chem. Phys.* **2010**, *211*, 727–735.
- (28) Lis, H.; Sharon, N. *Chem. Rev.* **1998**, *98*, 637–674.
- (29) Cairo, C. W.; Gestwicki, J. E.; Kanai, M.; Kiessling, L. L. *J. Am. Chem. Soc.* **2002**, *124*, 1615–1619.
- (30) Gestwicki, J. E.; Cairo, C. W.; Strong, L. E.; Oetjen, K. A.; Kiessling, L. L. *J. Am. Chem. Soc.* **2002**, *124*, 14922–14933.
- (31) Ghosh, R. J. *Chromatogr. A* **2002**, *952*, 13–27.
- (32) Zhou, J. X.; Tressel, T. *Biotechnol. Prog.* **2006**, *22*, 341–349.
- (33) Kalbfuss, B.; Wolff, M.; Geisler, L.; Tappe, A.; Wickramasinghe, R.; Thom, V.; Reichl, U. *J. Membr. Sci.* **2007**, *299*, 251–260.
- (34) Yang, Q.; Wu, J.; Li, J. J.; Hu, M. X.; Xu, Z. K. *Macromol. Rapid Commun.* **2006**, *27*, 1942–1948.
- (35) Yang, Q.; Hu, M. X.; Dai, Z. W.; Tian, J.; Xu, Z. K. *Langmuir* **2006**, *22*, 9345–9349.
- (36) Disney, M. D.; Seeberger, P. H. *Chem. Biol.* **2004**, *11*, 1701–1707.
- (37) Mateescu, A.; Ye, J.; Narain, R.; Vamvakaki, M. *Soft Matter* **2009**, *5*, 1621–1629.
- (38) Wang, J.; Dismar, F.; Hubbuch, J.; Ulbricht, M. *J. Membr. Sci.* **2008**, *320*, 456–467.
- (39) Zhang, X. Z.; Yang, Y. Y.; Chung, T. S.; Ma, K. X. *Langmuir* **2001**, *17*, 6094–6099.
- (40) Geismann, C.; Yaroshchuk, A.; Ulbricht, M. *Langmuir* **2007**, *23*, 76–83.
- (41) Friebe, A.; Ulbricht, M. *Langmuir* **2007**, *23*, 10316–10322.
- (42) Friebe, A.; Ulbricht, M. *Macromolecules* **2009**, *42*, 1838–1848.
- (43) He, D. M.; Sun, W.; Schrader, T.; Ulbricht, M. *J. Mater. Chem.* **2009**, *19*, 253–260.
- (44) Wang, J.; Faber, R.; Ulbricht, M. *J. Chromatogr. A* **2009**, *1216*, 6490–6501.
- (45) Narain, R.; Armes, S. P. *Biomacromolecules* **2003**, *4*, 1746–1758.
- (46) Perrier, S.; Haddleton, D. M. *Macromol. Symp.* **2002**, *182*, 261–272.
- (47) Haddleton, D. M.; Perrier, S.; Bon, S. A. F. *Macromolecules* **2000**, *33*, 8246–8251.
- (48) Kickelbick, G.; Reinohl, U.; Ertel, T. S.; Weber, A.; Bertagnolli, H.; Matyjaszewski, K. *Inorg. Chem.* **2001**, *40*, 6–8.
- (49) Matyjaszewski, K.; Xia, J. H. *Chem. Rev.* **2001**, *101*, 2921–2990.
- (50) Matyjaszewski, K.; Miller, P. J.; Shukla, N.; Immaraporn, B.; Gelman, A.; Luokala, B. B.; Siclován, T. M.; Kickelbick, G.; Vallant, T.; Hoffmann, H.; Pakula, T. *Macromolecules* **1999**, *32*, 8716–8724.
- (51) Jones, D. M.; Huck, W. T. S. *Adv. Mater.* **2001**, *13*, 1256–1259.
- (52) Xu, F. J.; Cai, Q. J.; Kang, E. T.; Neoh, K. G. *Langmuir* **2005**, *21*, 3221–3225.
- (53) Xu, F. J.; Zhao, J. P.; Kang, E. T.; Neoh, K. G.; Li, J. *Langmuir* **2007**, *23*, 8585–8592.
- (54) Yang, Q.; Xu, Z. K.; Dai, Z. W.; Wang, J. L.; Ulbricht, M. *Chem. Mater.* **2005**, *17*, 3050–3058.
- (55) Yang, Q.; Xu, Z. K.; Hu, M. X.; Li, J. J.; Wu, J. *Langmuir* **2005**, *21*, 10717–10723.
- (56) Yang, Q.; Wan, L. S.; Xu, Z. K. *Chin. J. Polym. Sci.* **2008**, *26*, 363–367.
- (57) Yang, Q.; Kaul, C.; Ulbricht, M. *Langmuir* **2010**, *26*, 5746–5752.
- (58) Yang, Q.; Strathmann, M.; Rumpf, A.; Schaule, G.; Ulbricht, M. *ACS Appl. Mater. Interfaces* **2010**, *2*, 3555–3562.